



Dependence of α -phase size on flow stress during dynamic recrystallization steady state in Ti60 alloy

Hui Li, Zhang-Long Zhao* , Hong-Zhen Guo, Yong-Quan Ning, Ze-Kun Yao, Kai Li

Received: 10 May 2015 / Revised: 6 July 2015 / Accepted: 10 July 2015 / Published online: 29 June 2016
© The Nonferrous Metals Society of China and Springer-Verlag Berlin Heidelberg 2016

Abstract The dependence of α -phase size on flow stress was characterized by a proposed kinetic model during dynamic recrystallization (DRX) steady state in Ti60 alloy. According to the isothermal compression tests, the influence of deformation parameters on the steady-state flow stress was analyzed and the constitutive equation was established to predict the steady-state flow stress under different deformation temperatures and strain rates. A power-law relationship between the DRX average grain size and steady-state flow stress with an exponent of -2 is obtained from the dynamic balance during DRX steady state. The effect of deformation parameters on α -phase size was observed through the microstructure after deformation, and the applicability of the model for Ti60 alloy was verified by the comparison between predicted and experimental data.

Keywords Dynamic recrystallization; Steady state; Grain size; Ti60 alloy; Hot deformation

1 Introduction

Titanium alloys have been extensively applied in aerospace industries due to their attractive combination of properties such as low density, high specific strength, excellent fracture toughness, superior corrosion and erosion resistance [1, 2]. In order to satisfy the requirements of the enhanced properties for aero-engine, near- α high-temperature titanium alloys which can be stably serviced for long time at elevated temperature have been explored competitively all

over the world in recent years [3, 4]. Dynamic recrystallization (DRX) is an effective method which can lead to a significant grain refinement during hot deformation and enhance the mechanical properties of metal and alloys [5–7]. As previous researches suggested that the steady-state grain size becomes independent of the initial grain size and is significantly dependent on the deformation conditions once DRX reaches a steady state at large strain [8–10]. A significant control of microstructural morphologies and mechanical properties of the final components can be achieved through appropriate selection of thermomechanical processing parameters, if the relationship between processing parameters and the DRX steady-state grain size is determined [11].

Ti60 alloy is a newly developed high-temperature Ti-alloy designed as an engine material to work at the temperature up to 600 °C. In recent years, the influence of processing parameters on flow behavior and the evolution of microstructures of Ti60 alloy have been discussed in a large number of researches [12–14]. However, little work about the evolution of the grain size in the steady state during the hot deformation of titanium alloys has been conducted. In present work, a kinetic model was established to quantitatively describe the relationship between average α -phase size and steady-state flow stress. And the applicability of the model for the Ti60 alloy was verified based on the data of isothermal hot compression tests at different deformation temperatures and strain rates.

2 Experimental

The material used in this investigation was Ti60 high-temperature Ti-alloy with the following chemical compositions: 6.14 wt% Al, 3.68 wt% Sn, 3.43 wt% Zr,

H. Li, Z.-L. Zhao*, H.-Z. Guo, Y.-Q. Ning, Z.-K. Yao, K. Li
School of Materials Science and Engineering, Northwestern Polytechnical University, Xi'an 710072, China
e-mail: zlzhao@nwpu.edu.cn

0.52 wt% Mo, 0.40 wt% Nb, 0.55 wt% Si, 0.96 wt% Ta and balance Ti. The β transus temperature of the alloy was measured to be 1318 K by using the metallographic observation method. Cylindrical specimens with a diameter of 8 mm and a height of 12 mm were machined from the as-received bar alloy. The original microstructure of the specimen is composed of the equiaxed alpha phases uniformly distributed in beta transformed matrix, as shown in Fig. 1. Isothermal compression tests were carried out on a Gleeble-3500 thermomechanical simulator at the deformation temperature range of 1233–1353 K, the strain rate range of 0.001–10.000 s⁻¹, and the height reduction of 50 %. All the specimens were heated with a constant heating rate of 5 K·s⁻¹, soaked for 5 min to eliminate the thermal gradient, and then compressed under a constant strain rate to the desired deformation degree. The true stress–strain curves were recorded automatically from load–stroke data in the hot compression process. Then, some typical compressed specimens were sectioned along the compression direction for metallographic examination. After being polished mechanically and etched in the Kroll's reagent, the exposed surfaces were observed by optical microscope (OM, OLYMPUS-PM3).

3 Results and discussion

3.1 Flow behavior

The typical true stress–strain curves of the Ti60 alloy under different deformation temperatures and strain rates are shown in Fig. 2. The characteristics of the flow curves are significantly dependent on the deformation parameters. The flow stress, the value of stress in the true stress–strain curves, is sensitive to temperature and strain rate, and decreases with the increase in temperature and the decrease in strain rate. As seen in the Fig. 2, the flow stress of Ti60 alloy rapidly increases to a maximum value (peak stress) and then

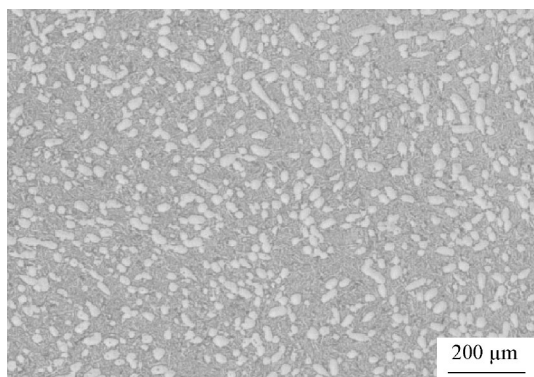


Fig. 1 OM image of initial microstructure of Ti60 alloy

gradually falls toward a relatively steady state, which can be concerned as the typical flow curve of DRX. At the beginning, stress increases constantly with the strain, and the feature of work hardening is observed. When strain reaches a certain value, the stress decreases as well as the alloy softens, since high strain energy accumulates too much inside the alloy, resulting in DRX. After an initial period of strain hardening, steady-state flow sets in at a strain, and the flow stress becomes steady due to the dynamic balance between softening and work hardening. And it is obvious that the variation of flow stress with strain becomes almost smooth and appears to be a steady state at a true strain of 0.6 for the isothermal compressed Ti60 alloy.

3.2 Constitutive equations for steady-state flow behavior

The correlation between the flow stress, strain rate and deformation temperature during hot deformation at a given strain can be expressed by an equation known as the Arrhenius-type relation as follows [15]:

$$\dot{\epsilon} = AF(\sigma) \exp(-Q/RT) \quad (1)$$

And the stress function of $F(\sigma)$ is defined by the following three forms:

$$F(\sigma) = \sigma^{n_1} \quad (\alpha\sigma < 0.8) \quad (2)$$

$$F(\sigma) = \exp(\beta\sigma) \quad (\alpha\sigma > 1.2) \quad (3)$$

$$F(\sigma) = \sinh(\alpha\sigma)^n \quad (\text{for all } \sigma) \quad (4)$$

where $\dot{\epsilon}$ is the strain rate (s⁻¹), σ is the flow stress (MPa), Q is the apparent activation energy for hot deformation (kJ·mol⁻¹), R is the gas constant, T is the deformation temperature (K), n and n_1 are the stress exponents, A , α and β are the material constants. According to Eq. (1), $\dot{\epsilon}$ can be described as:

$$\dot{\epsilon} = A[\sinh(\alpha\sigma)]^n \exp(-Q/RT) \quad (5)$$

Equation (5) can effectively describe the dependence of the temperature and strain rate on the steady-state flow stress. In general, the combined effects of deformation temperature and strain rate on the flow stress of alloys can be characterized by the Zener–Hollomon (Z) parameter, which can be expressed as [16]:

$$Z = \dot{\epsilon} \exp(-Q/RT) = A[\sinh(\alpha\sigma)]^n \quad (6)$$

Then, the flow stress can be written as a function of Z parameter, and the relation between them is as follows:

$$\sigma = \frac{1}{\alpha} \ln \left\{ \left(\frac{Z}{A} \right)^{\frac{1}{n}} + \left[\left(\frac{Z}{A} \right)^{\frac{2}{n}} + 1 \right]^{\frac{1}{2}} \right\} \quad (7)$$

According to these equations, after calculating the material constants (α , n , Q and A), the flow stress is then

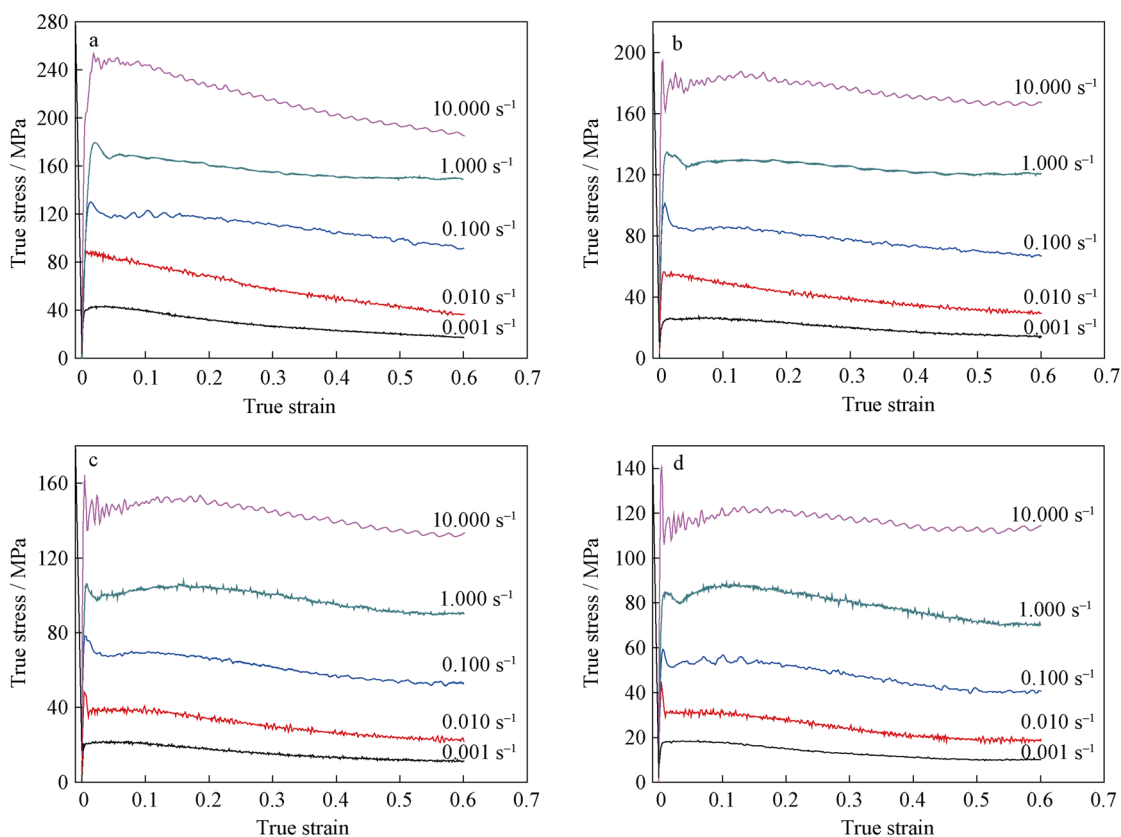


Fig. 2 Typical flow curves obtained from isothermal compression of Ti60 alloy at different temperatures: **a** 1233 K, **b** 1263 K, **c** 1293 K, and **d** 1333 K

obtained. These material constants can be obtained from the slopes of the linear fitting of relevant parameters, as seen in the Figs. 3 and 4. And the values of the above material constants at the strain of 0.6 are listed in Table 1. By substituting the values into Eq. (7), the steady-state flow stress (σ_{ss}) of Ti60 alloy can be calculated by the constitutive equation as:

$$\sigma_{ss} = 60 \times \ln \left\{ \left(\frac{Z}{5.21 \times 10^{15}} \right)^{\frac{1}{2.566}} + \left[\left(\frac{Z}{5.21 \times 10^{15}} \right)^{\frac{2}{2.566}} + 1 \right]^{\frac{1}{2}} \right\} \quad (8)$$

Figure 5 shows the flow stress of steady state in isothermal compression tests of the Ti60 alloy. As seen, the steady-state flow stress decreases with temperature increasing and

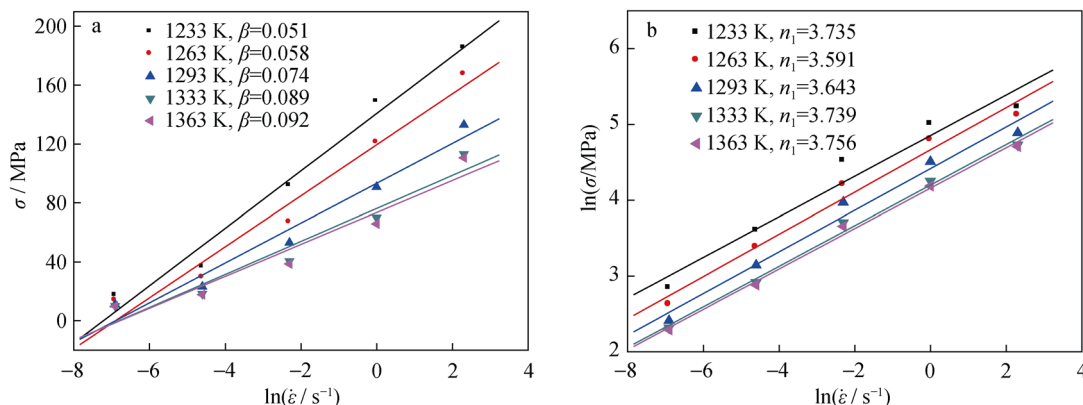


Fig. 3 Relationship between **a** σ and $\ln \dot{\epsilon}$, and **b** $\ln \sigma$ and $\ln \dot{\epsilon}$

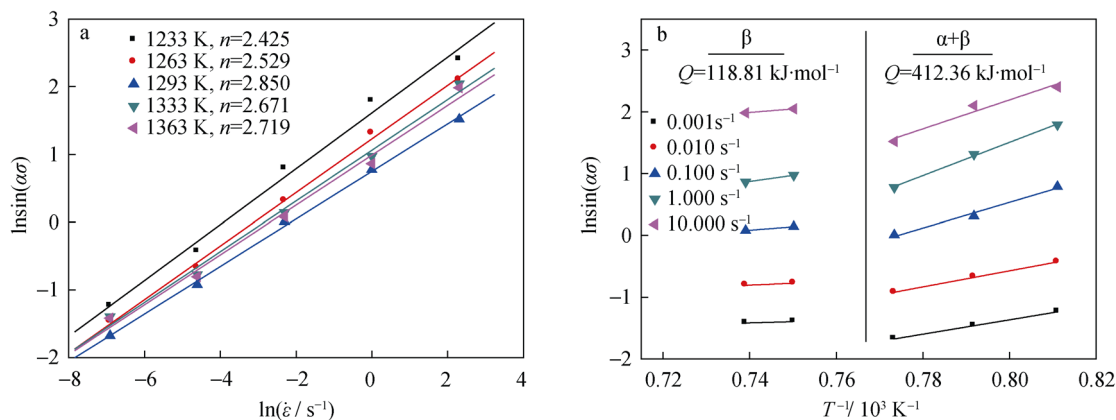


Fig. 4 Relationship of **a** $\ln \sin(\alpha\sigma)$ versus $\ln \dot{\epsilon}$, and **b** $\ln \sin(\alpha\sigma)$ versus $1000/T$

Table 1 Material constants at a strain of 0.6

| Phase field | β/MPa^{-1} | n_1 | α/MPa^{-1} | n | $Q/(\text{kJ}\cdot\text{mol}^{-1})$ | $\ln A$ |
|------------------|-------------------------|-------|--------------------------|-------|-------------------------------------|---------|
| $\alpha + \beta$ | 0.061 | 3.656 | 0.0167 | 2.566 | 412.36 | 36.19 |
| β | 0.091 | 3.747 | 0.0242 | 2.672 | 118.81 | 7.89 |

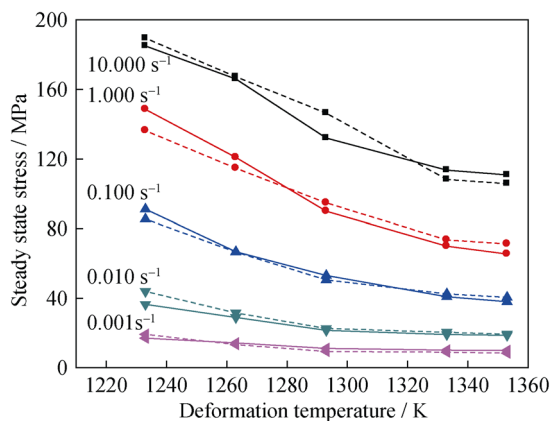


Fig. 5 Measured (solid line) and predicted (dotted line) steady-state flow stress in isothermal compression of Ti60 alloy

strain rate decreasing. And the flow stress decreases much more slightly with the increase in deformation temperature at low strain rates than at high strain rate. On the other hand, above the β transus temperature of Ti60 alloy, the steady flow stresses scarcely vary with the deformation temperature at low strain rates. The similar phenomenon was also observed in some other titanium alloys [17].

3.3 Steady-state grain size determination

It is well known that a steady state can develop during large strain deformation when DRX occurs. The steady-state grain size during DRX by grain boundary migration is

shown to be simply related to deformation stress for a number of metals and minerals. This state can be characterized by a constant flow stress (σ) and a constant average grain size (D). Derby [18] documented that these two parameters can be related to each other via a power-law relationship if the stress and the grain size are normalized by the shear modulus (μ) and the Burgers vector length (b), respectively:

$$\frac{\sigma}{\mu} = \frac{K}{(D/b)^n} \quad (9)$$

where K denotes a constant usually within the range from 1 to 10. In the present paper, the prediction for the evolution of grain size is based on the assumption that the grains expand in spherical shape. The Gibbs free energy change during nucleation is composed of two main terms. One is volumetric and represents the energy difference due to the elimination of the dislocations and preexisting grain boundaries by formation of the nucleus. The second term represents the energy rise by creation of additional grain boundary [19]. The global Gibbs free energy change (ΔG) is expressed by:

$$\Delta G = -P \cdot 4\pi r^2 dr + \gamma \cdot 8\pi r dr \quad (10)$$

where P is the unit volumetric energy change, γ is the grain boundary energy, and r is the radius of the grain. The grain boundary energy is a function of the misorientation of adjacent subgrains. The grain boundary energy of high angle boundary can be directly calculated by the Read–Shockley equation [20]

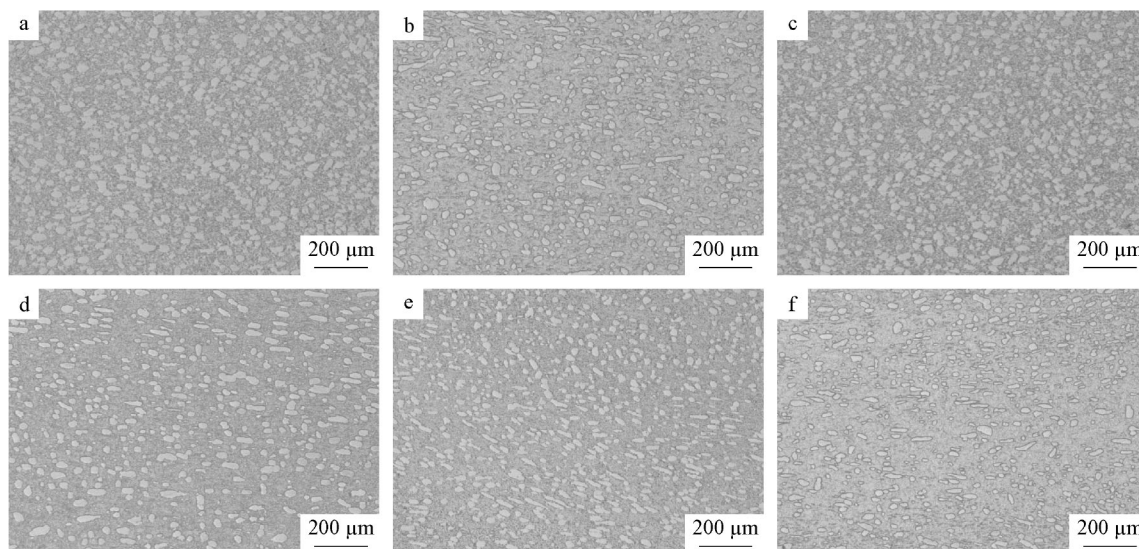


Fig. 6 OM images of Ti60 alloy at different temperatures and strain rates: **a** 1233 K, 0.001 s⁻¹; **b** 1263 K, 0.001 s⁻¹; **c** 1233 K, 0.010 s⁻¹; **d** 1263 K, 0.010 s⁻¹; **e** 1233 K, 0.100 s⁻¹; **f** 1263 K, 0.100 s⁻¹

$$\gamma = \frac{\mu b \theta}{4\pi(1 - \nu)} \tag{11}$$

where b is the burgers vector and ν and θ are respectively Poisson’s ratio and misorientation when the grain boundary becomes a high angle boundary (taken as 15°).

The unit volumetric energy change (P) depends on the dislocation density in the matrix and can be estimated as follows [11]:

$$P = \frac{1}{2} \rho \mu b^2 \tag{12}$$

where ρ is the dislocation density in the matrix. And μ is a temperature-dependent shear modulus (GPa), in form of [21]:

$$\mu = 49.02 - \frac{5.821}{e^{181/T} - 1} \tag{13}$$

At steady state, the volumetric energy change is equal to the surface energy of the nucleus. Therefore, Eq. (10) can be written as:

$$\Delta G = 0 \tag{14}$$

By combining the equations above, the radius of the grain can be expressed as:

$$r = \frac{4\gamma}{\rho \mu b^2} \tag{15}$$

In the one-parameter approach of Kocks and Mecking [22], the KM model, σ is expressed in terms of the dislocation density (ρ):

$$\sigma = M a \mu b \sqrt{\rho} \tag{16}$$

where a is Taylor constant and M is the average Taylor factor which relates the macroscopically imposed strain to

the total slip on all active glide systems in the grains. As reported before [23–25], the variation of M can be included in the model and was considered as constant for simplicity in this study. Then the relationship between the grain size (D) and the steady-state flow stress can be described by:

$$D = 8\gamma M^2 a^2 \mu \sigma_{ss}^{-2} \tag{17}$$

From Eq. (17), it can be seen that the average grain size is inversely proportional to the steady-state stress (σ_{ss}). And the derivational relationship between the flow stress and average grain size is similar to the Derby law. In the steady-state stage, the work hardening, the dynamic recovery and the DRX are in a dynamic balance, so that the stored energy maintains a constant value. As a result, DRX grain size (D) no longer changes with strain increasing. According to the constitutive equation, the steady-state flow stress (σ_{ss}) increases as the increasing of Z value which indicating an increase in stored energy. Consequently, the DRX average grain size (D) decreases because nucleation rate increases faster than growth rate [10].

Figure 6 shows the microstructures of specimens compressed in $\alpha + \beta$ phase field at different strain rates. As seen, the morphology of α phase is an equiaxed structure, and α phase is uniformly distributed in the matrix, which characterizes the progress of DRX. And the size of α phase is sensitive to the deformation conditions, which increases with deformation temperature increasing and strain rate decreasing. In order to verify the prediction accuracy of the above inverse power law, the relationship between the diameter of the α phase and the steady-state flow stress at the deformation temperature of 1233 and 1263 K was analyzed, as shown in Fig. 7. As seen, the result of the

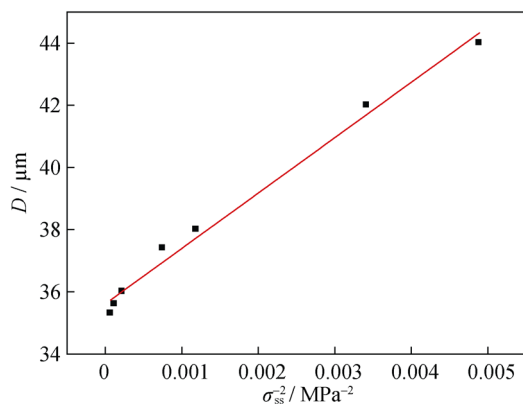


Fig. 7 Relationship between average grain size (D) and steady-state stress (σ_{ss}^{-2})

proposed model is in a good coincidence with the experimental result. And it indicates that the relationship among the size of grain or phase, steady-state flow stress and the deformation parameters during DRX steady state in Ti60 alloy can be relatively well described by the model.

4 Conclusion

The isothermal compression tests of Ti60 alloy were conducted to investigate the dependence of α -phase size on flow stress during DRX steady state. The constitutive equation was established to describe the effect of deformation conditions on the steady-state flow stress, which decreases with temperature increasing and strain rate decreasing. The correlation between DRX average grain size and steady-state flow stress is described by a power-law relationship with an exponent of -2 . And the model could be well used to predict the average α -phase size during the DRX in Ti60 alloy.

Acknowledgments This study was financially supported by the National Natural Science Foundation of China (No. 51205319), the Natural Science Foundation of Shanxi Province (No. 2015JQ5152) and the Fundamental Research Funds for the Central Universities (No. 3102016ZY010).

References

- [1] Weiss I, Semiatin SL. Thermomechanical processing of alpha titanium alloys—an overview. *Mater Sci Eng A*. 1999;263(2):243.
- [2] Wang YL, Hui SX, Liu R, Ye WJ, Yu Y, Kayumov R. Dynamic response and plastic deformation behavior of Ti–5Al–2.5Sn ELI and Ti–8Al–1Mo–1V alloys under high-strain rate. *Rare Met*. 2014;33(2):127.
- [3] Wanjara P, Jahazi M, Monajati H, Yue S. Influence of thermomechanical processing on microstructural evolution in near- α alloy IMI834. *Mater Sci Eng A*. 2006;416(1–2):300.
- [4] Ma FC, Lu WJ, Qin JN, Zhang D. Microstructure evolution of near- α titanium alloys during thermomechanical processing. *Mater Sci Eng A*. 2006;416(1–2):59.
- [5] Lin YC, Chen XM, Wen DX, Chen MS. A physically-based constitutive model for a typical nickel-based superalloy. *Comput Mater Sci*. 2014;83:282.
- [6] Chen XM, Lin YC, Wen DX, Zhang JL, He M. Dynamic recrystallization behavior of a typical nickel-based superalloy during hot deformation. *Mater Des*. 2014;57:568.
- [7] Al-Samman T, Gottstein G. Dynamic recrystallization during high temperature deformation of magnesium. *Mater Sci Eng A*. 2008;490(1–2):411.
- [8] Galindo-Nava EI, Rivera-Díaz-del-Castillo PEJ. Grain size evolution during discontinuous dynamic recrystallization. *Scr Mater*. 2014;72–73:1.
- [9] Cram DG, Zurob HS, Brechet YJM, Hutchinson CR. Modeling discontinuous dynamic recrystallization using a physically based model for nucleation. *Acta Metall*. 2009;57(17):5218.
- [10] Wang BX, Liu XH, Wang GD. Dynamic recrystallization behavior and microstructural evolution in a Mn–Cr gear steel. *Mater Sci Eng A*. 2005;393(1–2):102.
- [11] Momeni A, Ebrahimi GR, Jahazi M. Microstructure evolution at the onset of discontinuous dynamic recrystallization: a physics-based model of subgrain critical size. *J Alloys Compd*. 2014;587:199.
- [12] Zhao ZL, Li H, Fu MW, Guo HZ, Yao ZK. Effect of the initial microstructure on the deformation behavior of Ti60 titanium alloy at high temperature processing. *J Alloys Compd*. 2014;617:525.
- [13] Jia WJ, Zeng WD, Liu JR, Zhou YG, Wang QJ. On the influence of processing parameters on microstructural evolution of a near alpha titanium alloy. *Mater Sci Eng A*. 2011;530:135.
- [14] Peng WW, Zeng WD, Wang QJ, Yu HQ. Comparative study on constitutive relationship of as-cast Ti60 titanium alloy during hot deformation based on Arrhenius-type and artificial neural network models. *Mater Des*. 2013;51:95.
- [15] Lin YC, Chen XM. A critical review of experimental results and constitutive descriptions for metals and alloys in hot working. *Mater Des*. 2011;32(4):1733.
- [16] Sellars CM, McTegart WJ. On the mechanism of hot deformation. *Acta Metall*. 1966;14(9):1136.
- [17] Zhang XY, Li MQ, Li H, Luo J, Su SB, Wang H. Deformation behavior in isothermal compression of the TC11 titanium alloy. *Mater Des*. 2010;31(6):2851.
- [18] Derby B. The dependence of grain size on stress during dynamic recrystallisation. *Acta Metall Mater*. 1991;39(5):955.
- [19] Faver J, Fabrègue D, Piot D, Tang N, Koizumi Y, Maire E, Chiba A. Modeling grain boundary motion and dynamic recrystallization in pure metals. *Metall Mater Trans A*. 2013;44(13):5861.
- [20] Chen F, Cui ZS, Liu J, Chen W, Chen SJ. Mesoscale simulation of the high-temperature austenitizing and dynamic recrystallization by coupling a cellular automaton with a topology deformation technique. *Mater Sci Eng A*. 2010;527(21–22):5539.

- [21] Picu RC, Majorell A. Mechanical behavior of Ti–6Al–4V at high and moderate temperatures-part II: constitutive modeling. *Mater Sci Eng A*. 2002;326(2):306.
- [22] Mecking H, Kocks UF. Kinetics of flow and strain-hardening. *Acta Metall*. 1981;29(11):1865.
- [23] Estrin Y. Dislocation theory based constitutive modelling: foundations and applications. *J Mater Process Technol*. 1998; 80–81:33.
- [24] OuYang DL, Fu MW, Lu SQ. Study on the dynamic recrystallization behavior of Ti-alloy Ti–10V–2Fe–3V in β processing via experiment and simulation. *Mater Sci Eng A*. 2014;619: 26.
- [25] Roters F, Raabe D, Gottstein G. Work hardening in heterogeneous alloys—a microstructural approach based on three internal state variables. *Acta Mater*. 2000;48(17):4181.